High-Throughput 3D Visualization of Cell Proliferation within 3D Cell Culture Models.

Thomas S. Villani[1], Graeme Gradner[1], Michael T Johnson[1], Will Marshall[2]

[1]Visikol Inc, 675 US Highway 1, North Brunswick, NJ, 08902, [2]GE Healthcare Life Sciences, 1040 12th Ave NW, Issaquah, WA 98027

Abstract

Because of their improved *in vivo* relevancy compared to 2D monolayer cell culture models, 3D cell culture models are being rapidly adopted by researchers for use in basic research as well as the drug discovery pipeline. In studying these models, cell proliferation (e.g. Ki67) is a commonly used biomarker to assess the degree to which cells are being affected by compounds and antibodies. However, one of the challenges with current 3D cell culture characterization techniques is that one-dimensional assays lose spatial end-points, while traditional wide-field and confocal microscopy only characterize the periphery of these models due to light attenuation. This is problematic and biases data as only the periphery of these models is being used for characterization today in image-based end-point assays which bias results, as the exterior is most exposed to the compound of interest. It was shown that by combining a plate-compatible tissue clearing technique with laser high content confocal microscopy that entire 3D cell culture models could be characterized in their entirety. This ability to characterize all of the cells within these models allowed for the analysis of cell proliferation as a function of depth which provides useful information about the kinetics and penetration of compounds and antibodies.

Materials and Methods

HepG2 cells were cultured according to published techniques. Wells of Corning ULA U-bottom plates (Corning Cat. No. 4515) were seeded with 1,000 cells, and incubated with 5% CO_2 at 37°C for 2 days to form spheroids.

Treatment of spheroids with antiproliferative compound

Spheroids were treated with antiproliferative compound (paclitaxel) on day 0, and again on day 3. Paclitaxel was dissolved in DMSO, and from this stock solution, 10-fold serial dilutions were prepared to make 100x working dilutions. Compound was diluted to final assay concentration in growth media. The assayed concentrations were 1 µM, 500 nM, 100 nM, 10 nM, 1 nM, and vehicle control.

Fixation and immunolabeling

On day 5, spheroids were fixed using 10% NBF, followed by washing in PBS to remove fixative. Spheroids were treated with methanol, followed by 20% DMSO/methanol to improve penetration of antibodies and stains. Spheroids were blocked with 10% donkey serum. Spheroids were incubated with rabbit anti-Ki67 antibody (1:150 dilution) to label proliferating cells. Nuclei stained with DAPI (ThermoFisher).

Clearing and high throughput imaging of spheroids

Spheroids were cleared with Visikol HISTO-M. Imaging of spheroid plate was accomplished using a GE InCell 6000 High Content Confocal Imager. Z-stacks were collected for each tissue, using 5 µm steps. Images were processed using ImageJ, and DAPI+ and Ki67+ cells were counted using CellProfiler.

Results and Discussion

Visikol HISTO-M enables visualization of spheroid interior

As seen in Figure 2A, when imaging 3D tissue cultures, the interior of the spheroid appears dark, as light scattering drastically reduces signal due to the opacity of the spheroids. Using Visikol HISTO-M, light scattering was greatly reduced, allowing for comprehensive profiling of the interior of the spheroids, shown in Figure 2B.

Visikol HISTO-M increases detectable cells in interior

CellProfiler was used for automated cell-counting of the confocal image stacks. The data shown in Figure 3 illustrate the inherent problems with imaging non-cleared spheroids. The image stack progresses into the non-cleared spheroid, fewer and fewer cells are detected in each plane, until only the periphery is detectable. This is due to light scattering caused by the opacity of non-cleared spheroids, which limits imaging to approximately 20-50 µm, even with confocal microscopy. With cleared spheroids (Figure 3) cells are detectable across the entire image plane, deep into the spheroid. As can be seen in the graph, on average, 3-fold more cells were detected on each plane of the cleared spheroid than the non-cleared spheroid. The effect is even more dramatic deeper in the spheroid; at 120 µm 7-fold more cells were detectable.

When conducting confocal imaging of spheroids without clearing, only the outermost cells are detected due to light scattering reducing signal. Use of a tissue clearing agent greatly increases the number of cells detectable by high content imaging. Corning ultra-low attachment plates are chemically compatible with Visikol HISTO-M clearing, so generation of spheroid, labeling, and imaging can be conducted without transfer of spheroids. The clearing process takes only minutes, and is done within the wells.

Case study: Antiproliferative assay on HepG2 spheroids

Paclitaxel treated and control spheroids were imaged using a GE InCell 6000 High Content Imager to obtain multicolor image stacks with a 5 µm z-step size. Ki67 was used as a marker for proliferation. Cells were counted automatically with CellProfiler, giving total cell counts (DAPI+) and Ki67+ cell counts. Ki67+ cells were counted only if they colocalized with DAPI+ staining. Ki67%, the ratio of Ki67+ to total cells, was used as the measurement of proliferation. Dose response curves were constructed for cleared and non-cleared spheroids, shown in Figure 4. As can be easily discerned from Figure 4A, there was a significant measured difference between dose response curves constructed from cleared and non-cleared spheroids. The non-cleared spheroids demonstrated significantly higher apparent Ki67%--the outer layers of cells were the only detectable cells in non-cleared spheroids, and this population of cells exhibits a higher relative level of proliferation compared to the inner population of cells, as is reflected in the dose response curves for cleared spheroids. Since the entire cell population is measured in cleared-spheroids, the Ki67% measured is more representative of the spheroid population, since the inner, less-proliferative cells are included in measurements.

Spheroid Finder

If we consider a 96 well plate with a 2.6 mm well diameter and a spheroid that is 250 µm in diameter then the total well area is 5.3 mm^2 and the spheroid diameter is 0.05 mm^2. This ratio is important to understand for the high-throughput imaging of spheroids as conducting confocal imaging on the entire well would be incredibly time-consuming where a full plate would take 3 days. GE has developed a Spheroid Finder that automatically determines spheroid locations from a very fast low magnification scan of the entire plate. The instrument then follows up with a more detailed high resolution scan with fields of view centered only over areas that contain spheroids. In practice, for sparse but large samples this typically results in a 15000 fold reduction in scan time and overall data accumulation.

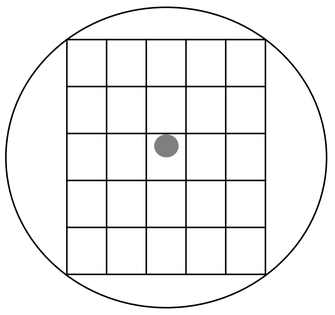

Figure 1. Diagram of spheroid in well plate.

For more accurate segmentation and quantification of cellular and subcellular structures in dense 3D cultures we plan to perform similar assays using the EDGE confocal imaging modality available on the IN Cell 6500. The technique provides a theoretical 2 fold increase in z-resolution and an order of magnitude increase in contrast over typical confocal imaging. The use of clearing and higher resolution imaging technologies that are compatible with multi-well plate assays could potentially allow for extraction of more descriptive phenotypic information from spheroids in addition to cell counts and overall integrated intensities.

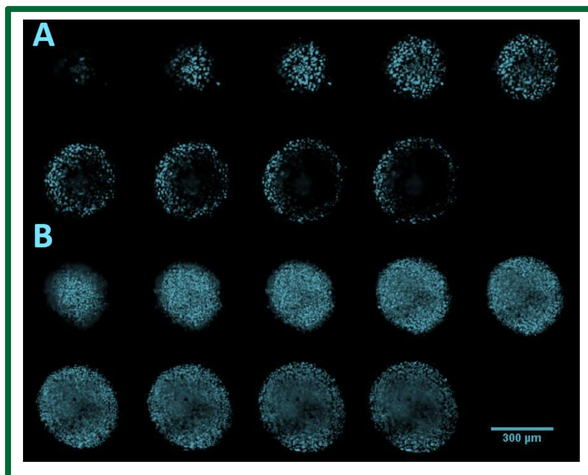

Figure 2. Montage of 20 µm slices from confocal image stack of nuclear-stained spheroid; A) Non-cleared spheroid; B) Cleared spheroid.

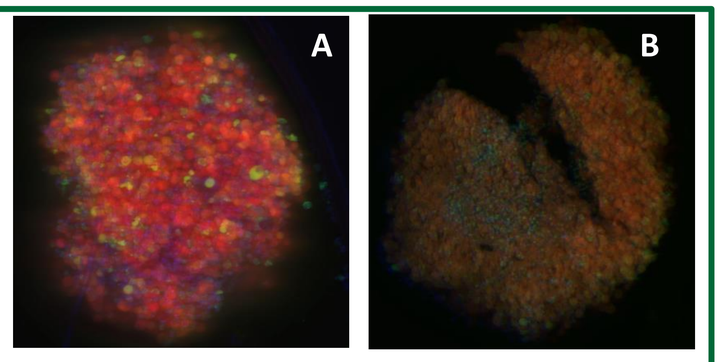

Figure 3. HepG2 spheroids stained with Calcein AM, DAPI and Propidium Iodide. A) Imaged with GE IN CELL 6500 using Iris confocal and B) Imaged with GE IN CELL 6500 using Edge confocal.

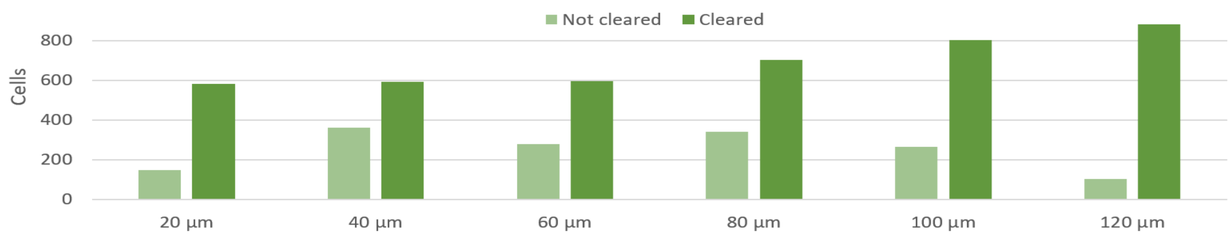

Figure 4. Cells detected at various z-depth through cleared and non-cleared HepG2 spheroids.

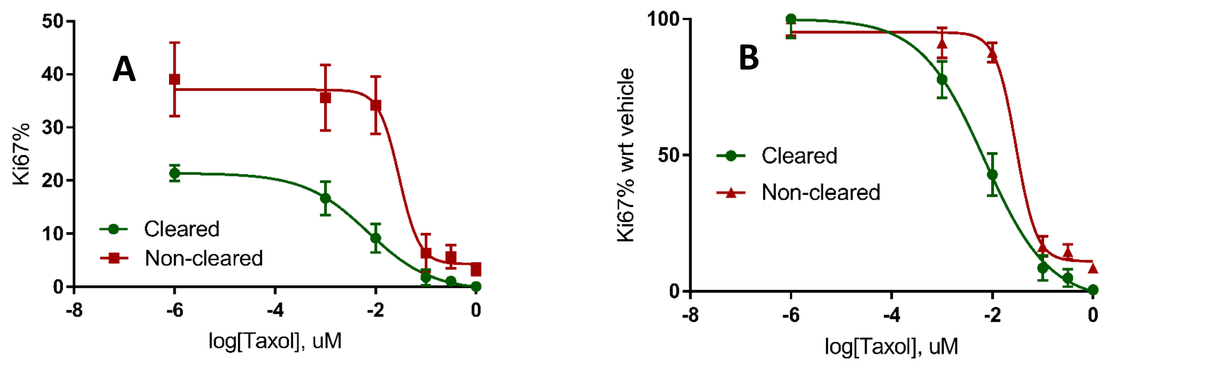

Figure 5. Ki67% dose response curves for cleared and non-cleared HepG2 spheroids. A) Absolute Ki67% dose response curve for paclitaxel-treated HepG2 spheroids; B) Dose response curves showing Ki67% with respect to vehicle Ki67% for paclitaxel-treated HepG2 spheroids.

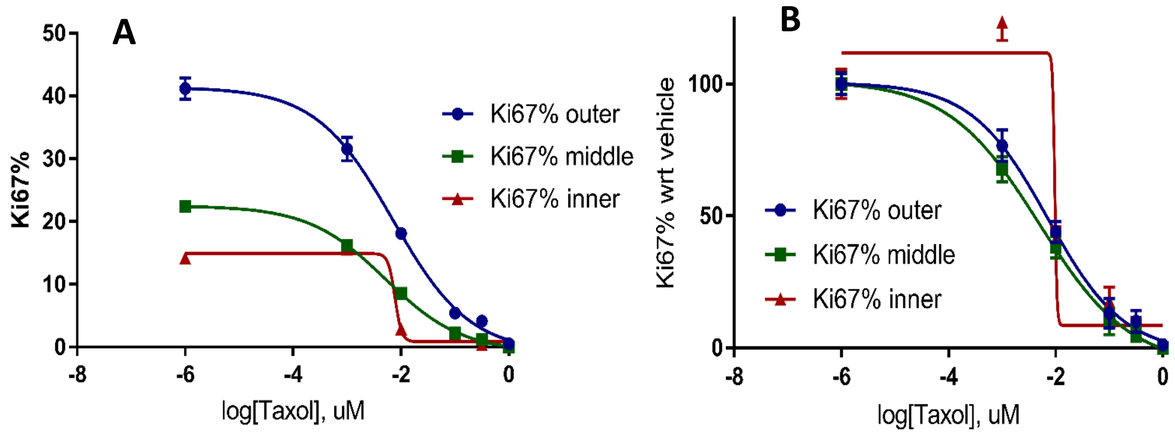

Figure 6. Spatial dose response curves for Ki67% measured in HepG2 spheroids. A) Absolute Ki67% dose response curves for three populations of cells in paclitaxel-treated HepG2 spheroids; B) Dose response curves showing Ki67% with respect to vehicle Ki67% for three populations of cells in paclitaxel-treated HepG2 spheroids.